Measurement of hyperfine coupling constants of the $5d\ ^2D_j$ levels in Cs using polarization quantum-beat spectroscopy

Wo Yei, A. Sieradzan,* E. Cerasuolo, and M. D. Havey
Physics Department, Old Dominion University, Norfolk, Virginia 23529
(Received 17 July 1997)

A precise measurement of the $5d\ ^2D_j$ ($j=\frac{3}{2},\frac{5}{2}$) hyperfine structure in atomic Cs is reported. A pump and delayed-probe method based on quantum-beat spectroscopy has been used, whereby the linear polarization degree of the probe signal is determined as a function of probe delay. From the measured polarization beat frequencies for delays up to about 180 ns, the magnetic-dipole and electric-quadrupole coupling constants A and B for the two levels are obtained: $A=-21.24(5)$ MHz and $B=0.2(5)$ MHz for the $5d\ ^2D_{5/2}$ level and $A=48.78(7)$ MHz and $B=0.1(7)$ MHz for the $5d\ ^2D_{3/2}$ level. [S1050-2947(98)02305-1]

PACS number(s): 32.10.Fn, 32.30.−r, 32.80.−t, 42.62.Fi

I. INTRODUCTION

There is currently considerable interest in accurate determinations of excited-state properties of atomic systems [1–5]. Among the factors motivating present studies is a range of basic physics or metrological applications associated with knowledge of such quantities as oscillator strengths and fine or hyperfine coupling constants [6–8]. In addition, advances in the sophistication of atomic structure calculations [9] have produced a fruitful experiment-theory synergy, leading to significant progress in the quality of both measurement and computation.

A general motivation for this work is to provide higher-quality data on hyperfine-structure and atomic transition matrix elements in the heavier alkali-metal atoms Rb and Cs. For these atoms, relativistic effects and core polarization lead to strong anomalies in fine-structure branching ratios and to inversions in the j-component energy ordering within fine-structure multiplets [10]. An additional motivation for this study is to provide precise hyperfine coupling constant measurements for comparison with elaborate calculations of various structural properties of cesium [11,12]. The calculations in turn are prompted by the need to remove atomic structural contributions from measurements of observables displaying atomic parity violation.

A variety of experimental techniques have been brought to bear on measurements of hyperfine coupling constants in the ground state of atoms, resulting in extraordinary precision in many cases [13–21]. However, the experimental situation for excited-state hyperfine coupling constants is generally less satisfactory, due partly to the limitations associated with the natural linewidth of the atomic transitions of interest. Subnatural linewidth resolution may then be required for accurate determination of hyperfine energy-level separations. To accomplish this, hyperfine quantum-beat spectroscopy can been applied, both in absorption and in emission, to the determination of hyperfine energy splittings of excited levels [6,22,23].

By using polarization hyperfine quantum-beat spectroscopy, our group has previously made precise measurements of the hyperfine structure of the resonance $np\ ^2P_{3/2}$ level in atomic ^{23}Na ($n=3$) [22] and ^{41}K ($n=4$) [23]. In addition, we have recently completed studies of the hyperfine structure of both the $3d\ ^2D_{3/2}$ and $3d\ ^2D_{5/2}$ levels of the isotopic sequence ^{39}K, ^{40}K, and ^{41}K [6]. The measurements in Na were extended to observation times greater than eight $3p\ ^2P_{3/2}$ radiative lifetimes, leading to subnatural resolution of the hyperfine structure. Subnatural resolution was exceptionally evident in the measurements in ^{41}K, where the manifold of hyperfine structure is obscured by the natural width of about 6 MHz.

The present study is concerned with measurements of hyperfine coupling constants in the atomic Cs $5d\ ^2D_j$ levels ($j=3/2,5/2$), for which we have determined the most precise values to date of the hyperfine coupling constants. However, the significantly larger hyperfine quantum-beat frequencies associated with the $5d\ ^2D_j$ levels, compared to those studied in previous experiments, put particular demands on the technique and indicate a general high-frequency boundary beyond which methods other than the hyperfine quantum-beat approach might be more usefully employed.

In the following sections the general plan and details of our experimental approach are presented. These are followed by the presentation and discussion of the experimental results and the method of analysis. A comparison of the measurements to previous determinations of the $5d\ ^2D_j$ hyperfine coupling constants is then made.

II. EXPERIMENT

The experimental approach is a modification of the hyperfine polarization quantum beats and delayed-detection methods described in previous papers [6,22,23]. The reader is referred to those reports for further details of the general scheme. Only those parts particular to the current measurements are described here. The general approach is illustrated in Fig. 1, which shows the excitation and detection scheme and relevant atomic cesium energy levels [24]. In the method, excitation of either the $5d\ ^2D_{5/2}$ or $5d\ ^2D_{3/2}$ level by a pulsed pump laser beam generates population and alignment in that level. For broadband excitation the hyperfine

*Permanent address: Physics Department, Central Michigan University, Mt. Pleasant, MI 48859.

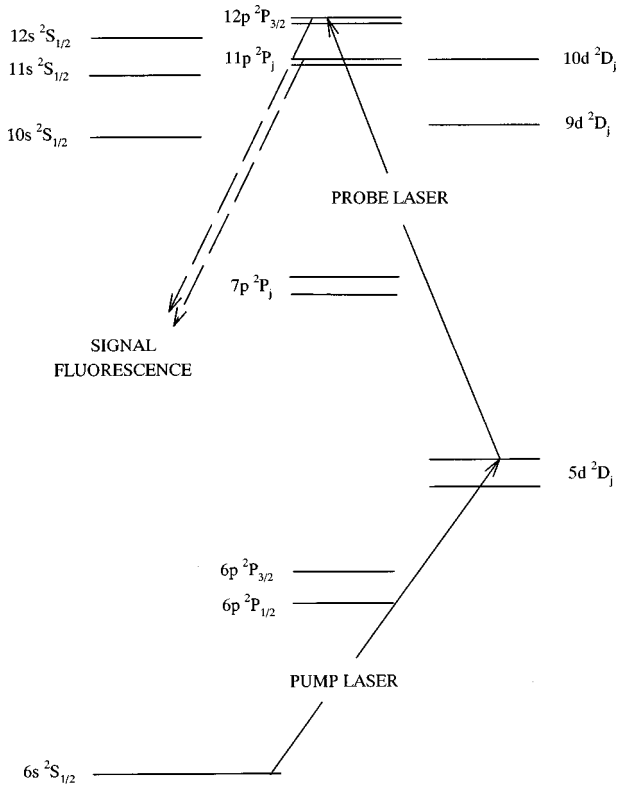

FIG. 1. Partial energy-level diagram for Cs, indicating the excitation and fluorescence cascade pathways.

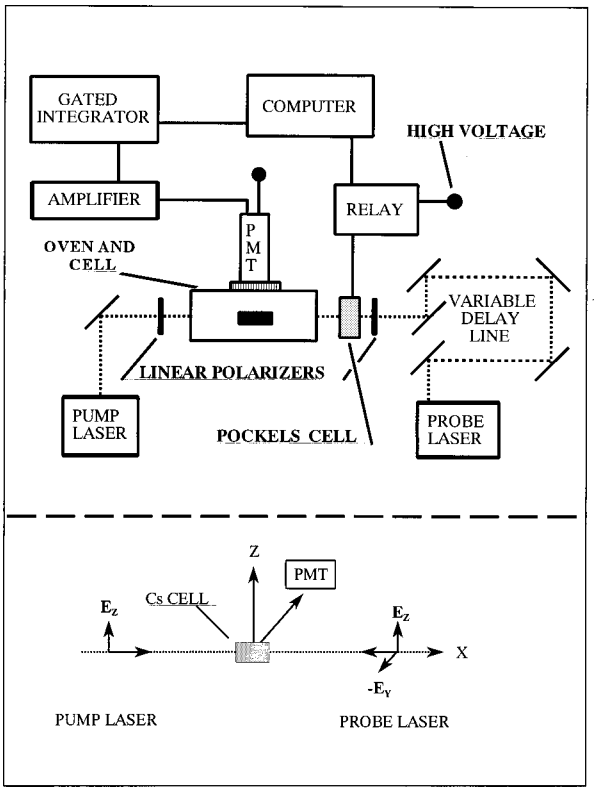

FIG. 2. Schematic diagram of the experimental apparatus. The inset shows the relative polarization directions of the pump and probe laser and the location of the detector.

levels are coherently excited and the hyperfine interaction modulates the alignment components at combinations of the hyperfine frequencies in the $5d\ ^2D_j$ levels. The components of the alignment are monitored by varying the time delay T, relative to the pump beam, of the absorption of a pulsed probe beam. Variation of the signals with T may be determined with the probe laser linearly polarized either parallel or perpendicular to the linear polarization direction of the pump beam. It is experimentally more convenient to measure both of these and to form a linear polarization degree from the measurements. This quantity is normalized at each delay T and thus is insensitive to many experimental variables, including variations in laser power and focusing, cesium density, and drifts in laser frequency over the course of a run. Fitting the modulated polarization versus T allows very accurate extraction of the hyperfine frequencies in the $5d$ levels.

A schematic diagram of the experimental apparatus, which is similar to one employed earlier in measurements of the atomic Na $3p\ ^2P_{3/2}$ hyperfine structure, is shown in Fig. 2. Also shown in an inset is the geometry defining the polarization and propagation directions for the pump and probe lasers. As indicated in the figure, the pump laser was tuned to a quadrupole-allowed transition to excite Cs atoms from the $6s\ ^2S_{1/2}$ ground level to the $5d\ ^2D_{3/2}$ or $5d\ ^2D_{5/2}$ levels. The wavelength of the pump pulse was either 689.6 or 685.0 nm. Absorption of the probe pulse, occurring after a delay time T, promoted the Cs atoms from the excited $5d\ ^2D_j$ level to the final $12p\ ^2P_{3/2}$ level through an electric-dipole transition at either 650.8 or 655.0 nm. Note that the entire pump-probe excitation scheme is a weak process, for the quadrupole pump transition rate is about 10^6 times smaller than that of the usual electric-dipole transition, with an oscillator strength on the order of 10^{-7} [25,26].

Both pump and probe lasers indicated in the figures were linearly polarized and tunable dye lasers were simultaneously pumped by a common 1-MW nitrogen gas laser, which generated ultraviolet output at 337.1 nm in nominally 0.6-ns pulses. The pulse repetition rate was about 5 Hz. The laser beams were weakly focused, with a diameter of about 1 mm in the interaction region, and were counterpropagating through the sample cell. Typical laser energies in the interaction region were about 5 μJ for both the pump and probe laser. A nominal dye laser pulse width was about 0.5 ns, while the spectral width of each laser was $\sim 3\ \mathrm{cm}^{-1}$, much larger than the combined width of the transitions due to Doppler or natural broadening. This ensured that the two-photon pump excitation was broad, for it encompassed the combined ground and excited level hyperfine splitting of about $0.30\ \mathrm{cm}^{-1}$. However, the lasers were sufficiently narrow to clearly resolve the final-state fine-structure splitting of about $12\ \mathrm{cm}^{-1}$ in the $12p\ ^2P_j$ level.

The probe linear polarization was switched from parallel to perpendicular to that of the pump after every five laser shots. Switching was achieved by passing the probe beam through a Pockels cell, which had a half-wave voltage of about 4850 V. The analyzing power of the resulting polarimeter was approximately 0.999.

The $12p\ ^2P_{3/2} \rightarrow 6s\ ^2S_{1/2}$ fluorescence at 334 nm and the subsequent $np \rightarrow 6s\ ^2S_{1/2}$ cascade fluorescence were used as a measure of the excitation rate for each probe polarization. These decay channels were selected by means of ultraviolet-transmitting colored glass filters placed in the detection arm

of the apparatus. The linear polarization degree P_L used to determine the $5d$ level hyperfine coupling constants was formed by measurement of the signal intensity for each orientation of the probe linear polarization direction ($I_\parallel$ and $I_\perp$). P_L was defined in the usual way as $P_L=(I_\parallel-I_\perp)/(I_\parallel+I_\perp)$. Signals were detected by a photomultiplier tube (PMT) operated in a gated-photon counting mode, with the 2-μs gate opening about 100 ns after the arrival of the probe pulse at the cell. Accumulated counts for each polarization channel were stored in a laboratory computer, which also controlled the Pockels cell switching. The cooled PMT had a dark counting rate of less than one count per 10^4 laser shots and background due to all other sources was negligible. Signal counting rate was normally less than 500 counts per 5000 laser shots, which was the length of a typical experimental run. The low counting rate minimized, but did not eliminate, the electronic dead time. Photon counting signals for each run were corrected for the dead time as necessary prior to determining the polarization for that run. In order to obtain a final statistical uncertainty of a few percent in the measured polarization, several runs were characteristically made at each delay time T and combined in the final analysis.

A critical measurement in determining the modulation frequencies is the delay time T, defined as the temporal interval between the arrival of the pump and probe pulses at the center of the cell. In the experiment, delay times of up to 180 ns were determined by directly measuring the path difference traversed by the laser pulses through an optical delay line and converting this to a time delay through the speed of light in air. The index of refraction of air under normal conditions (1.000 275 4) has a small, but not negligible, effect on the determination of T. The small differential shifts due to propagation through refractive elements such as polarizers, lenses, Pockels cell, and windows of the cell were accounted for by taking an index of refraction for these elements of 1.5. As described in detail in an earlier paper [22], mechanical determination with a surveying tape of the path length is exceptionally reliable and a single measurement may be determined to an accuracy of about $\frac{1}{8}$ in over a 100-ft measurement interval. Because our delay measurements were determined from a series of smaller distance intervals, which were then combined to give T, the total uncertainty in the delay time depends on the number of interval measurements. However, even for the longest delay time of about 180 ns, the uncertainty amounted to only about ± 0.04 ns. Finally, we point out that there is typically a shift of the overall time base due to the uncertainty in the shape of the individual pump and probe laser pulses. These shapes depend on characteristics of the dye lasers used, including alignment, dye concentration, and nitrogen pumping laser pulse shapes. The overall shift of typically 0.04 ns is treated as a fitting parameter in the data analysis and has a negligible effect on the determined hyperfine coupling constants.

III. RESULTS AND DISCUSSION

Excitation of the final $12p\ ^2P_{3/2}$ level proceeds via an $E2$-$E1$ stepwise process. The $E2$ excitation of the $5d\ ^2D_j$ levels generates population and alignment in those levels. Referring to the geometry of Fig. 2, the Cartesian form of the quadrupole operator is proportional to ZX, defining a plane of symmetry for the excitation process. The transition operator produces nonzero expectation values for two observable alignment components $\langle A_0\rangle$ and $\langle A_{2+}\rangle$ as defined in [27]:

$$\langle A_0\rangle=\frac{\langle 3J_z^2-J^2\rangle}{j(j+1)},\quad \langle A_{2+}\rangle=\frac{\langle J_x^2-J_y^2\rangle}{j(j+1)}. \tag{1}$$

Note that the optical excitation also generates fourth-rank tensor components. However, these components are not observable in the probing process via an $E1$ transition. For coherent excitation of the excited level hyperfine manifold, these second-rank tensor components evolve in time, under the influence of the hyperfine interaction, according to $\langle A_0(T)\rangle=g(T)\langle A_0(0)\rangle$ and $\langle A_{2+}(T)=g(T)\langle A_{2+}(0)\rangle$, where the common depolarization function $g(T)$ is given by [28]

$$g(T)=\sum_f\sum_{f'}[(2f+1)(2f'+1)/(2i+1)] \times W^2(j,f,j,f';i,2)\cos(\omega_{ff'}T). \tag{2}$$

Here $j=\frac{5}{2}$ or $\frac{3}{2}$ is the electronic angular momentum, $i=\frac{7}{2}$ is the Cs nuclear spin, and f is the total angular-momentum quantum number. $W(\,)$ is a Racah coefficient and the $\omega_{ff'}$ are the frequency separations between f and f' hyperfine levels. The summations are over f and f'.

The time evolution of the polarization, in the absence of other relaxation mechanisms or external fields, is then given by

$$P_L=\frac{3h(\langle A_0\rangle+\langle A_{2+}\rangle)}{[4+h(\langle A_0\rangle-3\langle A_{2+}\rangle)]}. \tag{3}$$

The quantity h, as defined in Blum [27], is dependent only on the initial and final values of the electronic angular momentum for the $E1$ probe transition. The values are given by $h=-\frac{7}{8}$ for the $5d\ ^2D_{5/2}\rightarrow 12p\ ^2P_{3/2}$ transition and by $h=1$ for the $5d\ ^2D_{3/2}\rightarrow 12p\ ^2P_{3/2}$ transition.

At $T=0$, the average multipole alignment components generated in the $5d\ ^2D_j$ levels are $\langle A_0\rangle=\langle A_{2+}\rangle=-\frac{16}{35}$ for the $j=\frac{5}{2}$ level and $\langle A_0\rangle=\langle A_{2+}\rangle=-\frac{2}{5}$ for the $j=\frac{3}{2}$ level. These values lead to linear polarization degrees at $T=0$ of $P_L(j=\frac{5}{2})=0.75$ and $P_L(j=\frac{3}{2})=-0.50$ for the two levels. The time evolution of P_L for the two levels then proceeds from these initial values. Mapping the T dependence of the polarization, which depends on the hyperfine frequencies in each level through $g(T)$, thus allows extraction of the frequencies from measurements of the polarization. Note that, in the absence of depolarizing effects in the $5d\ ^2D_j$ levels, the amplitude of the polarization beats is also determined by the expressions above. The adjustable parameters are the hyperfine coupling constants A and B for each level.

Polarization measurements for a total of 73 time delays were taken for mapping out the time dependence of the polarization of the $5d\ ^2D_{5/2}$ level. Measurements for 41 different delays were made for the $5d\ ^2D_{3/2}$ level. Each data point consists of a measured delay time, a polarization degree, and a calculated statistical error. As indicated earlier, the polarization degree at a delay time T is obtained by combining the data from several independent runs. The statistical error in

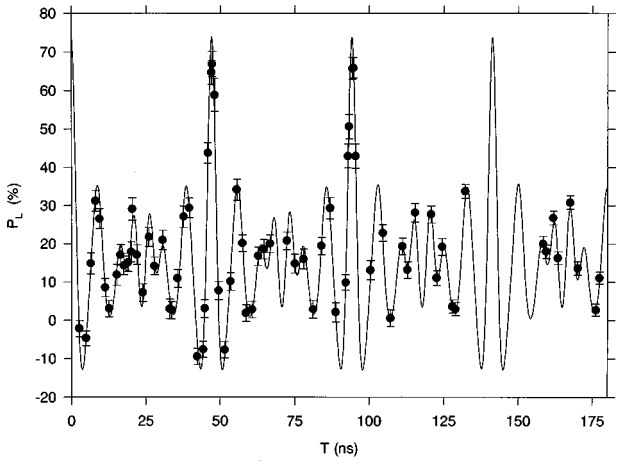

FIG. 3. Hyperfine polarization quantum beat data for the $5d\ ^2D_{5/2}$ level of Cs. The solid line represents the fit to the data.

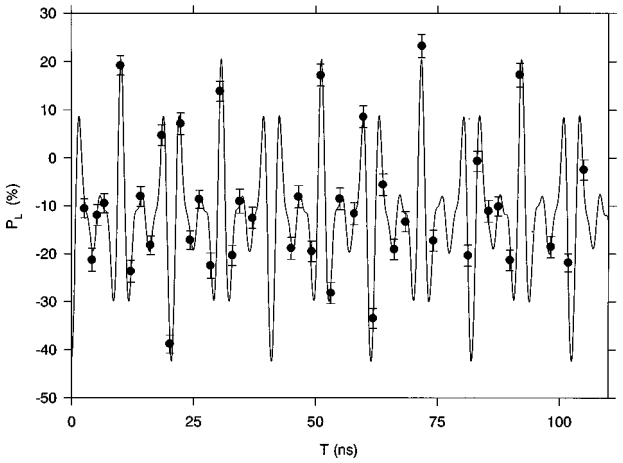

FIG. 4. Hyperfine polarization quantum beat data for the $5d\ ^2D_{3/2}$ level of Cs. The solid line represents the fit to the data.

the resulting P_L is obtained from the counting statistics of each run. Delay times for the $5d\ ^2D_{5/2}$ level ranged from 2.75 to 177.4 ns and for the $5d\ ^2D_{3/2}$ level from 2.67 to 104.9 ns. The photon counting signal for the $5d\ ^2D_{3/2}$ level was typically about 30% weaker than that of the $5d\ ^2D_{5/2}$ level and so more data runs at each delay were necessary to obtain comparable statistics for measurements on the two different multiplet levels. The experimentally obtained polarization spectra are shown in Figs. 3 and 4. The beats in the polarization are due to those in the alignment parameters and contain a number of frequencies determined largely by the magnetic coupling A for each level (for the quadrupole coupling B is very small). In the figures the vertical error bars shown represent the statistical errors in each P_L measurement, while the uncertainties in the individual delay times are negligible on the scale of the figures.

Considerable effort has been made in these experiments to minimize systematic effects. For the usual data-taking conditions, variations in pump and probe laser power, Cs density, and background counts had negligible effects on the measured polarization. It was possible to generate a reduction in P_L by a few percent by increasing the Cs density about a factor of 10 above the normal operating density; density effects were thus deemed negligible at the Cs density where data runs were made. The magnetic field in the interaction region of the cell was determined by a rotating coil magnetometer to be $\sim$30(30) mG. For this size of external magnetic field, no measurable Zeeman beats in the alignment during either the 2-μs measurement interval or the maximum $\sim$180-ns delay time were expected or observed. Finally, sealed atomic Cs sample cells were used in the experiment. In order to minimize collisional damping of the alignment in the $5d$ levels, the cells were prepared by baking at 460 K for 48 h at a base pressure of less than 10^{-7} Torr.

The main tools for analysis of the hyperfine polarization quantum beat signals are given in Eqs. (1)–(3). These expressions presume that the observable signals are proportional to the population produced in the $12p$ level. However, an important source of possible systematic modification of the polarization beat amplitudes, as given in the equations above, arises from the angular distribution of the $12p\ ^2P_{3/2} \rightarrow 6s\ ^2S_{1/2}$ fluorescence. As the probe polarization is varied to be parallel or perpendicular to that of the pump, the axis of alignment in the $12p\ ^2P_{3/2}$ level is rotated by 90°. The angular distribution of the intensity and polarization then changes for the two different probe directions. As the detector is fixed in space, the relative weights of the two intensities may be different than those leading to the expression for $P_L(T)$. The maximal size of this effect is greatly reduced by the hyperfine interaction in the $12p\ ^2P_{3/2}$ level, for this smooths the angular distribution of fluorescence. The imbalance in the two channels is further mitigated by the fact that a significant portion of the fluorescence signal arises from cascade fluorescence originating in the $11p$ and $10p$ levels. Estimates of this fraction show that the net effect should be small for the experiment described here. Finally, for a Cs density typical of a data run, significant depolarization of the $12p$ level due to Cs-Cs collisions is also expected. The above considerations suggest that effects due to the angular distribution of the decay fluorescence should be small. In fact, no statistically significant effect was apparent in the fit of the $5d\ ^2D_j$ polarization beat data to the $P_L(T)$ expression given above.

In order to fit the data presented in Figs. 3 and 4, a four-parameter, weighted least-squares-fitting procedure was

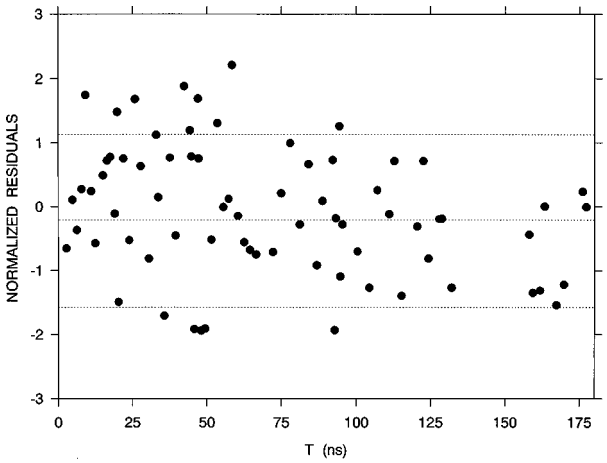

FIG. 5. Residuals of the fit of the analytical expressions to the polarization data for the $5d\ ^2D_{5/2}$ level. Values are normalized to the statistical uncertainty of each data point.

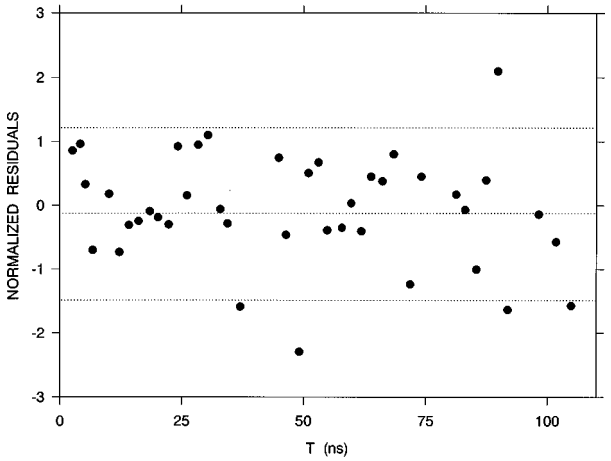

FIG. 6. Residuals of the fit of the analytical expressions to the polarization data for the $5d\ ^2D_{3/2}$ level. Values are normalized to the statistical uncertainty of each data point.

used. The parameters used were the hyperfine coupling constants A and B [8], the combined temporal width L of the pump and probe laser, and an overall shift δ in the delay time T. In the fit, the minimum in the reduced-χ^2 hypersurface was found. However, because the values of L and δ were quite well known to begin with, a simplified fitting procedure was employed. In it, the two parameters were held fixed at nominal values while A and B were varied to minimize the reduced χ^2. Then L and δ were in turn varied to search for a shift of the minimum. Of the parameters only the temporal width of the laser pulses was found to be statistically different from zero. For rectangular temporal laser pulses of width L, this quantity produces an overall phase shift for each oscillating term in the alignment given by $2\{[1-\cos(\omega_{ff'}L)]/(\omega_{ff'}L)^2\}$. Note that inclusion of L and δ did lead to a smaller reduced χ^2 for the fit and did reduce somewhat the derived uncertainty in A and B, but did not shift the obtained values of A and B outside the ultimate quoted uncertainty in the values. The simplified fitting procedure was not sensitive to variations in the order of fitting of the three other parameters or in the nominal starting values selected. Best-fit values for these parameters are $L=1.1(1.9)$ ns and $\delta=0.03(20)$ for the $5d\ ^2D_{5/2}$ level and $L=0.9(3)$ ns and $\delta=0.05(10)$ for the $5d\ ^2D_{3/2}$ level. The greater sensitivity to the laser pulse widths in the $5d\ ^2D_{3/2}$ level is a result of the higher beat frequencies in that case. To qualitatively illustrate the quality of the fit, normalized residuals are presented in Figs. 5 and 6, where the residual for each data point is defined as $[P_L(\text{fit})-P_L(\text{measured})]/\sigma$. The horizontal lines in the figures represent the mean residual and the $\pm 1\sigma$ boundaries. The mean residuals of $-0.02(12)$ for the $5d\ ^2D_{5/2}$ level and $-0.06(13)$ for the $5d\ ^2D_{3/2}$ level are consistent with 0 and the distribution of points is also consistent with a statistical distribution of residuals.

TABLE I. Summary of experimental determinations of the hyperfine coupling constants for the $5d\ ^2D_{5/2}$ and $5d\ ^2D_{3/2}$ levels in ^{133}Cs.

Parameter	Level	This work	Ref. [29]	Ref. [21]
A	$5d\ ^2D_{5/2}$	$-21.24(5)$	$-21.2(1)$	$-22.1(5)$
B	$5d\ ^2D_{5/2}$	0.2(5)	0.0(1.0)	
A	$5d\ ^2D_{3/2}$	48.78(7)	48.6(2)	
B	$5d\ ^2D_{3/2}$	0.1(7)	0.0(8)	

The final fitting parameters for the hyperfine coupling constants A and B for the $5d\ ^2D_j$ levels of Cs are summarized in Table I. Note that only the relative signs of A and B may be determined by the method; the signs are chosen to be consistent with other reported experimental results, which are also included in the table [21,29]. There it is seen that our results are consistent with others, but are several times more precise. This improvement in precision is characteristic of the method employed and was also seen in our earlier hyperfine-structure measurements on the transitions in Na and K. As discussed in an earlier paper, the limiting factor in this method is in the determination of the calibration of the delay-time base. For the results presented here, the higher-frequency oscillations in P_L occurring when A is ~ 50 MHz or so begin to establish practical limitations of the method as currently used. It seems that use of picosecond-pulse-length pump and probe lasers and possibly electronic calibration of the delay times using higher-frequency standard sources should increase the utility of the method to higher frequencies.

ACKNOWLEDGMENTS

The assistance of A. Beger in the early stages of this work is acknowledged. The financial support of the National Science Foundation is greatly appreciated.

[1] U. Volz and H. Schmoranzer, Phys. Scr. **T63**, 48 (1996).
[2] J. E. Simsarian, W. Shi, L. A. Orozce, G. D. Sprouse, and W. Z. Zhao, Opt. Lett. **21**, 1939 (1996).
[3] B. Hoeling, J. R. Yeh, T. Takekoshi, and R. J. Knize, Opt. Lett. **21**, 74 (1996).
[4] N. Ph. Georgiades, E. S. Polzik, and H. J. Kimble, Opt. Lett. **19**, 1474 (1994).
[5] D. Sundholm and J. Olsen, Phys. Rev. Lett. **68**, 927 (1992).
[6] A. Sieradzan, R. Stoleru, Wo Yei, and M. D. Havey, Phys. Rev. A **55**, 3475 (1997).
[7] J. Sagle and W. A. van Wijngaarden, Can. J. Phys. **69**, 808 (1991).
[8] E. Arimondo, M. Inguscio, and P. Violino, Rev. Mod. Phys. **49**, 31 (1977).
[9] For a recent summary of results on alkali atom lifetimes, see Ref. [1].
[10] T. F. Gallagher, *Rydberg Atoms* (Cambridge University Press, Cambridge, 1994).
[11] V. A. Dzuba, V. V. Flambaum, A. Ya. Kraftmakher, and O. P. Sushkov, Phys. Lett. A **142**, 373 (1989).

[12] S. A. Blundell, W. R. Johnson, and J. Sapirstein, Phys. Rev. A **43**, 3407 (1991).
[13] G. D. Stevens, Chun-Ho Iu, S. Williams, T. Bergeman, and H. Metcalf, Phys. Rev. A **51**, 2866 (1995).
[14] W. A. van Wijngaarden, J. Li, and J. Koh, Phys. Rev. A **48**, 829 (1993).
[15] W. A. van Wijngaarden and J. Sagle, Phys. Rev. A **43**, 2171 (1991).
[16] M. Głodź and M. Kraińska-Miszczak, Phys. Lett. A **160**, 85 (1991).
[17] W. A. van Wijngaarden and J. Sagle, J. Phys. B **24**, 897 (1991).
[18] R. Alheit, X. Feng, G. Z. Li, R. Schreiner, and G. Werth, J. Mod. Opt. **39**, 411 (1992).
[19] M. Głodź and M. Kraińska-Miszczak, J. Phys. B **18**, 1515 (1985).
[20] Carol E. Tanner and Carl Wieman, Phys. Rev. A **38**, 1616 (1988).
[21] L. K. Lam, R. Gupta, and W. Happer, Phys. Rev. A **21**, 1225 (1980).
[22] W. Yei, A. Sieradzan, and M. D. Havey, Phys. Rev. A **48**, 1909 (1993).
[23] A. Sieradzan, P. Kulatunga, and M. Havey, Phys. Rev. A **52**, 4447 (1995).
[24] A. A. Radzig and B. M. Smirnov, *Reference Data on Atoms, Molecules, and Ions* (Springer-Verlag, Berlin, 1985).
[25] Alan Corney, *Atomic and Laser Spectroscopy* (Oxford University Press, Oxford, 1988); E. Biemont and C. J. Zeippen, J. Phys. IV, 209 (1991).
[26] For example, A. Lindgard, and S. E. Nielsen, At. Data Nucl. Data Tables **19**, 6 (1977); B. Warner, Mon. Not. R. Astron. Soc. **139**, 115 (1968).
[27] K. Blum, *Density Matrix Theory and Application* (Plenum, New York, 1981).
[28] C. H. Greene and R. N. Zare, Annu. Rev. Phys. Chem. **33**, 119 (1982).
[29] K. Fredriksson, H. Lundberg, and S. Svanberg, Phys. Rev. A **21**, 241 (1980).